One-pot nanofibrillation of cellulose and nanocomposite production in a twin-screw extruder

M N F Norrrahim[1], H Ariffin[1,2*], T A T Yasim-Anuar[2], M A Hassan[1], H Nishida[3*], T Tsukegi[4]

[1]Department of Bioprocess Technology, Faculty of Biotechnology and Biomolecular Sciences, Universiti Putra Malaysia, 43400 UPM Serdang, Selangor, Malaysia.
[2]Laboratory of Biopolymer and Derivatives, Institute of Tropical Forestry and Forest Products (INTROP), Universiti Putra Malaysia, 43400 UPM Serdang, Selangor, Malaysia.
[3]Department of Biological Functions and Engineering, Graduate School of Life Science and Systems Engineering, Kyushu Institute of Technology, 2-4 Hibikino, Wakamatsu-ku, Kitakyushu, Fukuoka, 808-0196, Japan.
[4]Innovative Composite Materials Research and Development Center (ICC), Kanazawa Institute of Technology, Hakusan, Ishikawa 924-0838, Japan.

[*]Corresponding authors: hidayah@upm.edu.my (H Ariffin), nishida@lsse.kyutech.ac.jp (H Nishida)

Abstract. Oil palm mesocarp fiber (OPMF) is rich in cellulose and suitable to be used as raw material for the production of cellulose nanofiber (CNF) and biocomposite. Recently, there have been reports on the use of CNF as filler in polypropylene (PP) for improving the mechanical properties of PP, however the process requires two steps: (i) nanofibrillation for CNF production and (ii) biocomposite compounding. In this study, a one-pot process was developed whereby nanofibrillation of cellulose and subsequently melt-blending of the CNF with PP were conducted at once, in a twin-screw extruder. Morphological analysis of the biocomposites by SEM showed that the cellulose was successfully fibrillated into CNF and compounded homogeneously with PP. The highest tensile strength, Young's modulus, flexural strength, and flexural modulus recorded were 34.9 ± 0.5 MPa, 12.1 ± 0.1 GPa, 59.3 ± 1.3 MPa, and 2.3 ± 0.05 GPa, respectively when 3 % CNF was used in the biocomposite. The reinforcement of CNF-OPMF in PP improved the mechanical properties of the biocomposite by 33.4 % compared to neat PP. It is interesting to note that the addition of CNF managed to improve the crystallinity of the biocomposite (54.6 %) compared to neat PP (50.1 %), despite of the lower crystallinity of CNF compared to PP. This observation can be attributed to the high density of covalent bonds per cross-sectional area and the large number of hydrogen bonding sites. Additionally, the observation can be explained by the role of CNF in composite which acted as nucleation agent, which eventually increased the crystallinity of the biocomposite.

1. Introduction

Cellulose nanofiber (CNF) from renewable biomass has attracted much interest as an alternative to micro-sized reinforcement materials in composite plastics. There have been significant advances in the development of plant-plastic composites [1]. Owing to its high stiffness, it can be used to increase the mechanical strength of general-purpose thermoplastics such as polypropylene (PP), polyethylene (PE),

polyvinyl chloride, polylactic acid and nylon. PP is the most important and widely used polyolefin [2]. Its low density, low production cost, design flexibility, and recyclability make it a popular choice as a matrix for composite making. PP is hydrophobic, leading to compatibility issues when fillers with polar surfaces such as cellulose, are used.

A challenge when using CNF in biocomposites is due to its non-uniform dispersion. This is contributed by their polar surfaces which is difficult to disperse uniformly in a non-polar medium. This might be the reason why the processing of CNF biocomposites was first limited to solvent casting, where water soluble or dispersive polymers were the most common matrices [3]. However, the development of other, more flexible and industrially viable processing techniques is necessary to promote commercialization of these materials. Therefore, several interesting processing methods have been recently reported for these materials. One of the developed processing methods is melt compounding [4]. Melt compounding of cellulose nanocomposites presents several challenges [3]. The major difficulties in melt compounding are to feed the CNF into the extruder and achieve uniform dispersion in the polymer matrix. The CNF has high surface area and has tendency to aggregate when dried. This is expected to be avoided by firstly mixing them in a suitable medium, which is then fed into the extruder. Another method to provide uniform dispersion of nanocellulose in polymer matrix is by using solvent casting, nevertheless the process is not industrially applicable.

Reinforcement of CNF in PP by extrusion was discovered by Hassan et al. (2014) [5]. However, the fibrillation of cellulose into CNF was conducted separately from the extrusion. Based on results obtained, the mechanical properties of PP/CNF composites were improved as compared to neat PP. Furthermore, the reinforcing effects of CNF was better in the injection molded composites as compared to compression molded composites.

One-pot nanofibrillation of cellulose and compounding process for biocomposite production could be done by extrusion. The advantage of this kind of processing lies on its efficient production of CNF biocomposites due to fewer processing steps involved. The ability to blend CNF with PP by melt compounding using an extruder would be advantageous for large scale biocomposites production since extrusion will allow for high solid content processing and provide a continuous process. In this study, nanofibrillation of cellulose for the production of CNF and subsequently melt compounding of the CNF with PP was taken place in the same vessel, *i.e.* a twin-screw extruder. The biocomposites produced were characterized for their mechanical, morphological, crystallinity and thermal properties.

2. Materials and methods

2.1 Materials

OPMF was collected from Seri Ulu Langat Palm Oil Mill, Dengkil, Selangor. The fibers were first disintegrated, washed and dried. Sodium chlorite ($NaClO_2$) and potassium hydroxide (KOH) were obtained from ACROS ORGANICS and J.T Baker Neutracit, respectively.

2.2 Fiber treatment

In order to disintegrate the OPMF fibers physically, they were washed, cleaned, sorted and sun dried. Thereafter, pretreatment of fibers was conducted to recover the cellulose by removing hemicellulose and lignin in a method as explained below.

Lignin removal: Delignification was conducted by treating the OPMF with 5 wt% of sodium chlorite ($NaClO_2$) aqueous solution. pH of the solution was adjusted to pH 5 and the fibers were soaked in this solution at 70 ^{o}C for 1.5 hour. Then the fibers were washed and filtered with deionized water until the pH became neutral [6]. Following that, fibers were oven dried overnight.

Hemicellulose removal: KOH pretreatment was conducted by chemically treating the fibers with KOH to completely remove hemicellulose. Initially, fibers were dissolved in 6 wt % of KOH for 24 hours with constant stirring rate [6]. Sample was then filtered and rinsed with deionized water until to reach the pH=7.

Chemical composition of untreated and treated OPMF was shown in Table 1. More than 99% of cellulose was isolated from treated OPMF.

Table 1. Chemical composition of untreated and cellulose-OPMF

	Chemical composition * (%)		
Oil palm mesocarp fiber	**Cellulose**	**Hemicellulose**	**Lignin**
Untreated	38.38 ± 1.21	36.74 ± 1.59	24.88 ± 0.59
Cellulose-OPMF	99.46 ± 0.21	0.00 ± 0.00	0.54 ± 0.69

*Data provided is mean of triplicate samples

2.3 One-pot nanofibrillation and nanocomposite production in a twin-screw extruder

Fibrillation and melt compounding were carried out using a twin-screw extruder (Imoto machinery Co. Limited: Model IMO-160B). The extruder consisted of two major parts: fibrillation and mixing. Fibrillation of cellulose was conducted with a specially designed screw element: tooth-mixing elements (TME) for nanofibrillation at 120 ºC, with screw speed of 100 rpm for 1 hour [7]. After nanofibrillation was completed, the rotational speed was reduced to 25 rpm. This is to allow the movement of the fibrillated cellulose into mixing part. PP was fed through a hopper in between fibrillation and mixing section with the ratio of PP to cellulose of 97:3, 98:4 and 95:5. For melt compounding, temperature used was 180 ºC and screw speed was set at 25 rpm for 30 minutes. PP/CNF-OPMF composites were then pressed at the same temperature in an electrically heated platen press for 5 min under a pressure of 10 atm to form composite sheets.

2.4 Analysis

2.4.1 Visual examination. The visual appearance analysis of composites was conducted by using digital camera. Composites film were placed on the black fabric in order to avoid reflections. Therefore, a clear dispersion of CNF in composites can be observed. Pictures were taken in order to investigate the distribution of CNF in PP matrix.

2.4.2 Morphological analysis. The morphology of the CNF and the fracture surfaces of the composite samples were observed using SEM (FE-SEM S-3400N, Hitachi, Japan). Composites fracture surfaces were obtained through flexural tests. The dried CNF and fracture surfaces were coated with Pt-Pd for 100 s (Ion sputter: Hitachi, Japan) before the observations.

2.4.3 Mechanical properties. Tensile and flexural tests were performed to determine the mechanical properties of the composites using a mechanical tester (AGS-5kNG, Autograph, Shimadzu Co, Kyoto, Japan). Three-point flexural tests were performed on the bar-shaped composites samples at a crosshead speed of 5 mm/min; the span length for the tests was 50 mm. Flexural tensile (MPa) and flexural modulus (MPa) were obtained in this test. The dumbbell-like composites samples were subjected to tensile tests. The tensile tests were performed at a crosshead speed of 10 mm/min. Results of tensile strength (MPa), young's modulus (MPa), and elongation at break (%) were recorded.

2.4.4 Crystallinity analysis. X-ray diffraction (XRD) pattern was recorded using X-ray powder diffractometer (Rigaku Corporation, Tokyo, Japan) equipped with nickel filtered CuKα radiation (k= 0.1542 nm) at 40 kV and 25 mA. The diffractograms were detected in the range $2\theta = 2 - 50^{o}$ at a scan rate of 2º/min.

2.4.5 Differential scanning calorimetry analysis. Differential scanning calorimetry (DSC): measurements were performed using a Pyris 1 DSC calorimeter (Perkin–Elmer Co., Waltham, MA, USA). The samples were first heated from 30 to 200 °C at a rate of 10 °C/min and held at 200 °C for 1 min. They were then cooled to 50 °C at a rate of 10 °C/min and held at 50 °C for 1 min. Next, they were again heated to 200 °C at a rate of 10 °C/min and held at 200 °C for 1 min. Finally, they were quenched to 135 °C at a rate of 50 °C/min to determine their $\tau 1/2$ values. The temperatures corresponding to the exothermic and endothermic peaks in the first heating step and the cooling step were called T_m and T_c,

respectively. ΔH_m values were determined from the areas of the melting and crystallization peaks, respectively. The ΔH_m values was converted on the basis of the PP weight ratio of the composites.

2.4.6 Thermal stability. Thermal stability analysis was determined by using Thermo Gravimetry Analyser (TGA) (TGA – 9, Perkin Elmer, USA) under nitrogen flow. Sample (5-11 mg) was placed on a ceramic pan and set on the TGA. The sample was heated at heating rate of 10 ^{o}C min^{-1} within the temperature range of 50–550 ^{o}C.

3. Results and Discussion

3.1 Degree of fibrillation by extrusion

The effectiveness of nanofibrillation of cellulose-OPMF into CNF-OPMF by extrusion was evaluated and depicted in Figure 1. The SEM micrograph shows that the fibrillation did not occur when less than 3 % of fiber used. Small amount of fiber used gives a low force in the fibrillation part of extrusion which reduced the degree of fibrillation. In spite of this, only small amount of fiber was managed to move into nanocomposite part after fibrillation process completed when less than 3 % of fiber used. The fibrillated fiber was moved into the composite production part after the RPM of the extrusion screws was slow down to 25 RPM. However, as the amount of fiber increased, the fibrillation was increased. Fibrillation was occurred very well at 3% of cellulose as shown in Figure 1 (c). At higher magnification, the size of CNF was identified as <50 nm (Figure 1 (d)). Therefore, in this study, composites were produced from 3 % to 5 % of CNF to PP.

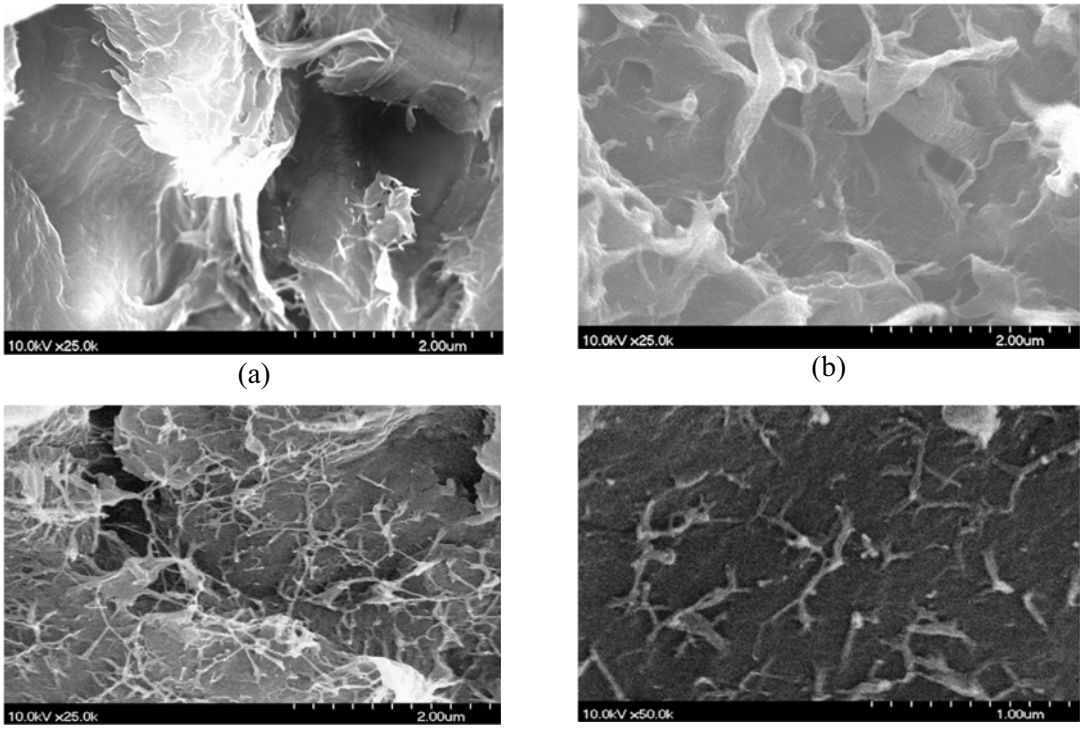

Figure 1. Morphology of fibrillated cellulose-OPMF by extrusion, (a) cellulose-OPMF (1%), (b) cellulose-OPMF (2%), (c) cellulose-OPMF (3%), (d) cellulose-OPMF (3%) (50,000 magnification).

3.2 Visual appearance

Visual appearance of the composites samples was observed to determine dispersion characteristic of CNF-OPMF in the PP matrix. It was seen that CNF in PP/CNF-OPMF (3%), PP/CNF-OPMF (4%), and PP/CNF-OPMF (5%) was well dispersed as shown in Figures 2 (a), (b) and (c). However, aggregation of CNF was observed in some parts of PP/CNF-OPMF (5%) composite (Figure 2 (c)). The aggregated CNF in PP matrix could be correlated to the decrement of the mechanical properties when CNF amount

was increased. In order to support this finding, morphological analysis of composites by SEM was also evaluated.

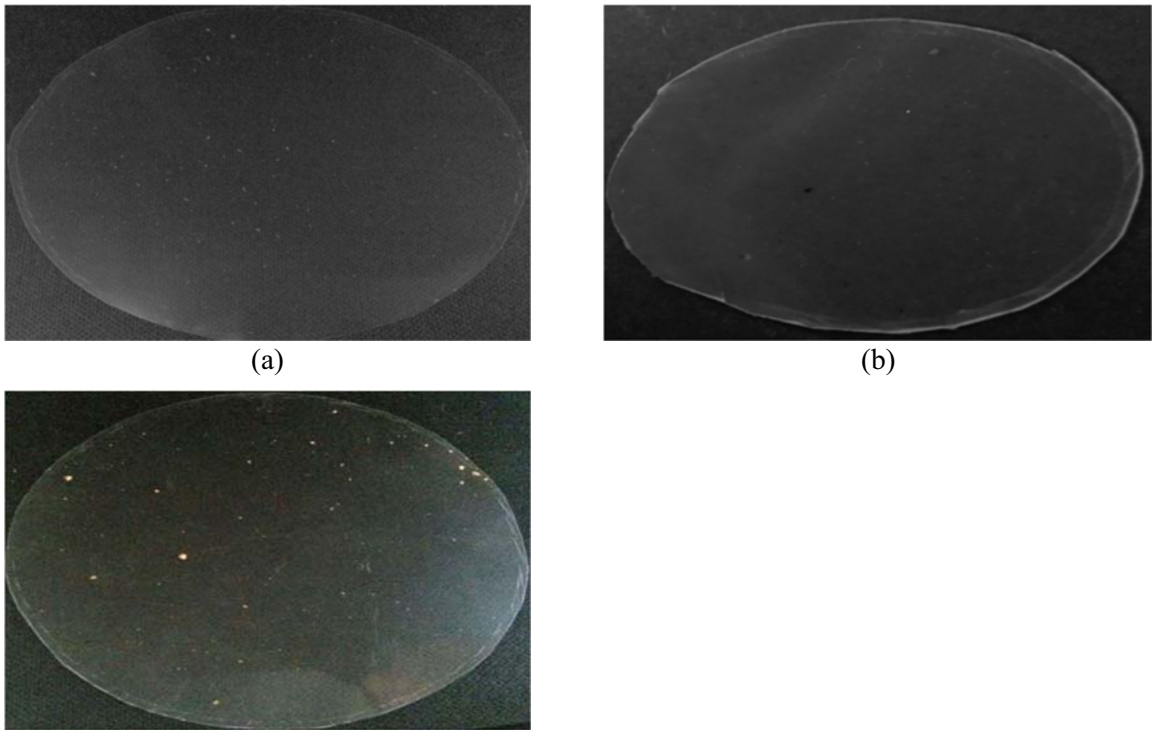

(a) (b)

(c)

Figure 2. Visual appearance of composites, (a) PP/CNF-OPMF (3%), (b) PP/CNF-OPMF (4%), (c) PP/CNF-OPMF (5%)

3.3 Morphological analysis

In correlation to the visual appearance analysis, morphology of the fractured sample of composites were analysed and depicted in Figure 3. For nanocomposite, it is difficult to identify the dispersion of CNF in the matrix. This is because the CNF was used in small amount and it was fully embedded within the PP matrix. Therefore, element detector system was also used to analyse the oxygen element based on chemical structure of celluloses as an indication for the dispersion of CNF in the matrix. Addition of 3 % CNF-OPMF in PP matrix results a homogeneous dispersion of CNF. There was only small amount of aggregations of oxygen element were observed. However, at 4 % and 5 % of CNF in PP matrix as shown in Figure 3 (b) and (c), aggregations of oxygen element were increased and clearly observed. This is concurrent with the visual appearance, where clear white spots of aggregated CNF were observed in the film. As discussed before, these aggregations indicated a limited chemical interaction between PP and CNF-OPMF which decrease the compatibility.

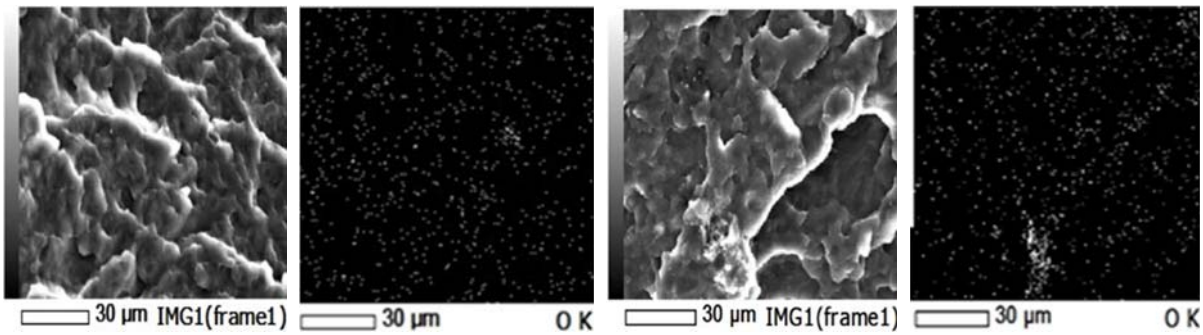

(a) (b)

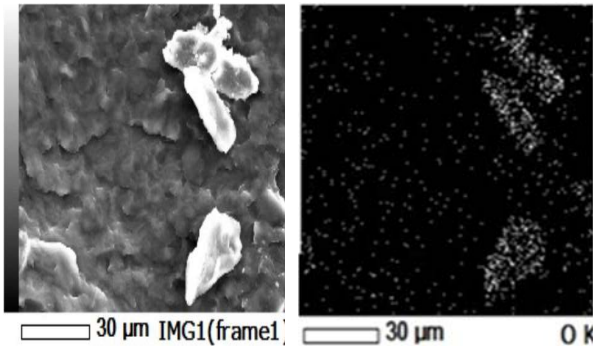

(c)

Figure 3. Micrograph of composites, (a) PP/CNF-OPMF (3%), (b) PP/CNF-OPMF (4%), (c) PP/CNF-OPMF (5%)

3.4 Mechanical properties

Mechanical properties of PP/CNF-OPMF composites and neat PP are shown in Table 2. The addition of CNF-OPMF to PP were markedly increased the tensile and flexural properties as compared to neat PP. For an example, tensile strength of PP/CNF-OPMF (3%) is 34.88 ± 0.5 MPa, as compared to neat PP 25.99 ± 0.5 MPa. Moreover, flexural strength of PP/CNF-OPMF (3%) was 59.32 ± 1.3 MPa as compared to neat PP 46.43 ± 0.8 MPa.

Table 2. Tensile and flexural properties of composites

Composites	Tensile strength (MPa)	Young's Modulus (MPa)	Elongation at break (%)	Flexural stress (MPa)	Flexural modulus (MPa)
Neat PP	25.99 ± 0.5	4394 ± 53	162 ± 13	46.43 ± 0.8	1237 ± 27
PP/CNF-OPMF (3 %)	34.88 ± 0.5	12121 ± 117	145 ± 8	59.32 ± 1.3	2337 ± 55
PP/CNF-OPMF (4 %)	31.49 ± 1.1	9386 ± 547	140 ± 7	53.06 ± 1.0	2201 ± 23
PP/CNF-OPMF (5 %)	29.01 ± 0.8	8315 ± 645	122 ± 5	42.75 ± 0.3	1609 ± 68

The Young's modulus and Flexural modulus of composites were significantly higher as compared to neat PP. The Young's modulus of PP/CNF-OPMF (3 %) was increased to 12121 ± 117 MPa as compared to neat PP 4394 ± 53 MPa. Meanwhile, the Flexural modulus of PP/OPMF-CNF (3 %) was 2337 ± 55 MPa as compared to neat PP 1237 ± 27 MPa. Since CNF is highly crystalline and tougher than neat PP, its influenced the increment on tensile and flexural properties of the composites than neat PP. In spite of this, these improvements can be attributed to the high density of covalent bonds per cross-sectional area and the large number of hydrogen bonding sites between CNF and PP.

Besides, as the amount of CNF increased in the composites, the mechanical strength was decreased. This is related to the dispersion of CNF in PP as discussed before. Aggregation of CNF could lead a poor stress transfer in the polymer matrix which resulted the decrement of the mechanical properties of PP/CNF-OPMF (4%) and PP/CNF-OPMF (5%).

3.5 Crystallinity properties

In order to support the mechanical properties analysis, crystallinity analysis was also conducted and depicted in Figure 4. High crystalline of CNF helps to improve the crystallinity of composites. This was due to the CNF acts as nucleation agent for crystallization occurs (Iwamoto *et al.,* 2014). As the amount of CNF increased, the crystallinity of the composites was also increased. The crystallinity of PP/CNF-OPMF (3 %), PP/CNF-OPMF (4 %), and PP/CNF-OPMF (5 %) were 54.64 %, 56.21 % and 57.00 % respectively as compared to neat PP 50.12 % (Table 3). Composites samples had higher crystallinity than neat PP which resulted in better mechanical properties as discussed before. Nevertheless, even though PP/CNF-OPMF (5 %) had the highest crystallinity, the mechanical properties of the composite sample were lower compared to PP/CNF-OPMF (3 %), which may explain that aggregation of CNF and eventually low stress transfer mainly affected the mechanical properties.

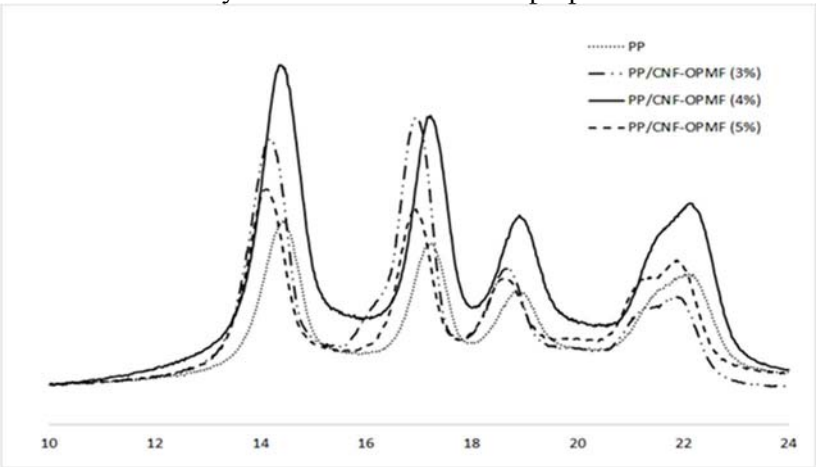

Figure 4. Crystallinity of composite samples.

Table 3. Crystallinity properties of composites.

Composition	Crystallinity (%)
Neat PP	50.12
PP/CNF-OPMF (3 %)	54.64
PP/CNF-OPMF (4 %)	56.21
PP/CNF-OPMF (5 %)	57.00

3.6 Thermal properties

Table 4 lists the thermal properties of PP/CNF-OPMF composites. The T_m values were almost similar in all samples, indicating that the CNF blended well with the polymer matrix. However, the T_c and ΔH_m of the composites were slightly higher than that of the neat PP, inferring that the crystallinity of the PP matrix in the composites was higher than that of the neat PP. This is correlate to the crystallinity analysis, where composites have higher crystallinity than neat PP. As the amount of CNF increased, T_c and ΔH_m were also increased. This is also indicated that the crystallization of the PP matrix in the composites started earlier in a non-isothermal cooling process than the neat PP.

Table 4. Thermal properties of composites.

Composition	*T*m (°C)	Δ*H*m (°C)	*T*c (°C)
Neat PP	162.23	99.2	116.59
PP/CNF-OPMF (3 %)	162.21	105.4	117.89
PP/CNF-OPMF (4 %)	162.24	106.1	118.32
PP/CNF-OPMF (5 %)	161.27	107.2	118.55

3.7 Thermal stability analysis

Thermal stability analysis of composites was analysed and depicted in Figure 5. It has been reported that cellulose acts as a nucleating agent [8], suggesting the presence of an interaction between cellulose and PP sequence. The interaction with solid materials must limit the mobility of polymers even at higher temperatures than melting points. Thus, the thermal stability of composites must be influenced by the crystallinity of PP in the composites. As the crystallinity of the composites prepared by one-step extrusion method was increased as compared to neat PP, the thermal stability based on the $T_{d50\%}$ were also increased. the $T_{d50\%}$ for PP/CNF-OPMF (3 %), PP/CNF-OPMF (4 %) and PP/CNF-OPMF (5 %) were 436.9 ºC, 444.1 ºC, and 449.3 ºC respectively, as compared to neat PP 426.8 ºC (Table 5). These results are correlated to the crystallization of PP enhanced by CNF in the composites as discussed before. Looking at different angle, the composites had more amorphous regions, which are easy to degrade compared to crystalline regions. Therefore, it also caused the neat PP easier to be decomposed than the composites.

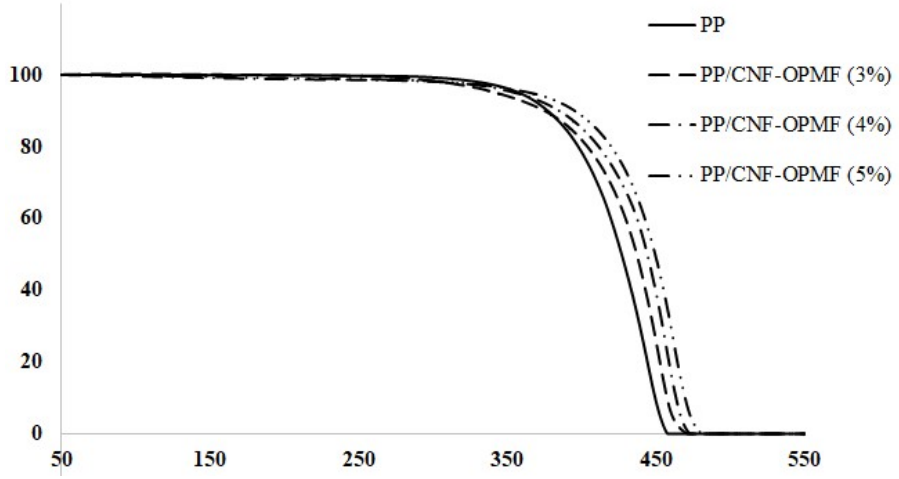

Figure 5. Thermal stability of composites.

Table 5. Thermal properties of composites.

Composition	$T_{d50\%}$ (ºC)
Neat PP	426.8
PP/CNF-OPMF (3 %)	436.9
PP/CNF-OPMF (4 %)	444.1
PP/CNF-OPMF (5 %)	449.3

4. Conclusions

A one-pot nanofibrillation of cellulose-OPMF and PP/CNF-OPMF composites processing was successfully developed by using a twin-screw extruder. The advantage of using a twin-screw extrusion process is that it allows for the processing and fibrillation of cellulose at high solid content. To the best of our knowledge, there is lack of research on one-pot nanofibrillation of cellulose and nanocomposite production by extrusion, and this report provides extensive information on the potential use of the method for PP/CNF-OPMF composite production. From our results, the morphological observation of PP and its composites showed that a relatively good dispersion of CNF was achieved as no CNF aggregates was visible in the fractured surfaces of the PP/CNF-OPMF (3%). CNF started to aggregate at higher concentration (5 wt%). Evaluation of the mechanical properties of the PP/CNF-OPMF composites showed that the composite samples had higher tensile and flexural properties compared to neat PP. The improvement in mechanical properties of the composite samples could be related to the high crystallinity of PP/CNF-OPMF. Nevertheless, despite of steady increment in crystallinity with the increased amount of CNF, the mechanical properties of the composite samples with higher CNF content

reduced slightly, mainly due to the CNF aggregation which resulted in low stress transfer. Generally speaking, the ability to fibrillate and produce the composite from CNF-OPMF by one-step extrusion method as proposed herewith, is possible to be commercialised due to its fast, simple and easy technique.

Acknowledgements
The authors gratefully acknowledge the Ministry of Higher Education Malaysia (MOHE) for financial support through SATREPS funding (vote no: 6300156) and the Ministry of Science, Technology and Innovation (MOSTI) for the provision of scholarship (MyPhD) to the first author. Authors also would like to acknowledge Japan International Cooperation Agency (JICA) for travel grant to Kyushu Institute of Technology, Japan.

References

[1] Iwamoto S, Yamamoto S, Lee S H, Endo T 2014 Solid-state shear pulverization as effective treatment for dispersing lignocelluloses nanofibers in polypropylene composites. *Cellulose* **21** 573-1580
[2] Hearle J W S 2001 Textile Fibers: A comparative Overview. *Encyclopedia of Materials: Science and Technology (Second Edition)* 9100-9116
[3] Oksman K, Aitomaki Y, Mathew A P Siqueira G Zhou Q Butylina S Tanpichai S Zhou X Hooshmand S 2016 Review of the recent developments in cellulose nanocomposite processing. *Compos Part A-Appl S* **83** 2-18
[4] Ho T T T, Abe K, Zimmermann T, Yano H 2015 Nanofibrillation of pulp fibers by twin-screw extrusion. *Cellulose* **22** 421-433
[5] Hassan M L, Mathew A P, Hassan E A, Fadel S M, Oksman K 2014 Improving cellulose/polypropylene nanocomposites properties with chemical modified bagasse nanofibers and maleated polypropylene. *J Reinf Plast Comp* **33** 26-36
[6] Nordin N I A A, Ariffin H, Ando Y, Hassan M A, Shirai Y, Nishida H, Yunus W M Z W, Karuppuchamy S, Ibrahim N A 2013 Modification of Oil Palm Mesocarp Fiber Characteristic Using Superheated Steam Treatment. *Molecules* **18** 9132-9146
[7] Nishida H, Yamashiro K, Tsukegi T 2017 Biomass Composites from Bamboo- Based Micro / Nanofibers, in *Handbook of Composite from Renewable Materials*. V. K. Thakur, M. K. Thakur, and M. R. Kessler, eds., Scrivener Publishing LLC, pp. 339–361
[8] Quillin D T, Caulfield D F, Koutsky J A 1993 Crystallinity in the polypropyrene/cellulose system. I. Nucleation and crystalline morphology. *J Appl Polym Sci* **50** 1187-1194
[9] Wang H W, Zhou H W, Gui L L, Ji H W, Zhang X C 2014 Analysis of effect of fiber orientation on Young's modulus for unidirectional fiber reinforced composites. *Compos Part B-Eng* **56** 733-739